

Two-Photon Fluorescence Microscopy Observation of Shape Changes at the Phase Transition in Phospholipid Giant Unilamellar Vesicles

L. A. Bagatolli and E. Gratton

Laboratory for Fluorescence Dynamics, University of Illinois at Urbana-Champaign, Urbana, Illinois 61801 USA

ABSTRACT Using the sectioning effect of the two-photon fluorescence microscope, we studied the behavior of phospholipid giant unilamellar vesicles (GUVs) composed of pure diacylphosphatidylcholine phospholipids during the gel-to-liquid crystalline phase transition. We used the well-characterized excitation generalized polarization function (GP_{ex}) of 6-dodecanoyl-2-dimethylamine-naphthalene (LAURDAN), which is sensitive to the changes in water content in the lipid vesicles, to monitor the phase transition in the GUVs. Even though the vesicles do not show temperature hysteresis at the main phase transition, we observed different behaviors of the vesicle shape, depending on how the GUV sample reaches the main phase transition. During the cooling cycles, we observed an increase in the vesicle diameter at the phase transition ($\sim 0.5\text{--}1\%$), followed by a decrease in the diameter when the vesicle reached the gel phase. During the heating cycles and close to the phase transition temperature, a surprising behavior is observed, showing a sequence of different vesicle shapes as follows: spherical-polygonal-ellipsoidal. We attribute these changes to the effect of lipid domain coexistence on the macroscopic structure of the GUVs. The “shape hysteresis” in the GUVs is reversible and largely independent of the temperature scan rate. In the presence of 30 mol% of cholesterol the events observed at the phase transition in the GUVs formed by pure phospholipids were absent.

INTRODUCTION

A common question about cell membranes is how the physical properties of lipid molecules can influence the structure and function of this many-particle two-dimensional molecular arrangement. The study of the physical and chemical properties in artificial lipid systems, where the lipid composition and the environmental conditions (such as temperature, ionic strength, pH, etc.) can be systematically controlled, provides information about the behavior of the lipid matrix. A process that has received great attention in the artificial lipid systems is the lipid main phase transition ($L_\alpha \rightarrow L_\beta$) induced by temperature. The phospholipid main phase transition has attracted theoretical and experimental attention, mainly because the phase transition reflects lipid-lipid interactions. Theoretical calculations were done using computer models to study the phospholipid main phase transition (Mouritsen and Zuckermann, 1985; Mouritsen, 1991). Moreover, an array of experimental techniques has been used to study the lipid phase transition, such as differential scanning calorimetry, fluorescence spectroscopy, NMR, x-ray diffraction, infrared spectroscopy, and electron spin resonance (Mabrey and Sturtevant, 1976; Eppand, 1995; Davenport and Targowski, 1995; Gratton and Parasassi, 1995; Parasassi and Gratton, 1995; McElhaney, 1982; Mason, 1998; Mantsch and McElhaney, 1991; Watts and Spooner, 1991). A useful experimental data review regarding the phases and phase transitions of the phosphatidylcholine-containing membranes was recently made by Koynova

and Caffrey (1998). The characteristics of the lipid samples, such as size, lamellarity, and shape, are strongly dependent on the method used to form the vesicles (Lasic, 1988). As a consequence of the preparation method, the parameters that characterize the main phase transition of lipids are affected by the lipid sample characteristics. Because of their cell dimensions and because of the possibility of directly observing single vesicles under the microscope, the giant unilamellar vesicles (GUVs) are becoming an object of intense scrutiny in diverse areas that focus on membrane behavior (Menger and Keiper, 1998). For example, Käs and Sackmann studied the shape transitions induced by area-to-volume changes of GUVs formed by synthetic phospholipids in the liquid crystalline state, using optical microscopy (Käs and Sackmann, 1991). Morphological changes induced by temperature were found in protein free lipid vesicles formed by bovine brain sphingomyelins (Döbereiner et al., 1993), showing how the intrinsic physical properties of the lipid membrane can play an important role in the naturally occurring budding and fission processes of the cell membranes. The mechanical properties of model membranes have been an object of intense study by the use of GUVs (Evans and Kwok, 1982; Needham et al., 1988; Needham and Evans, 1988; Meléard et al., 1997, 1998; for reviews see Sackmann, 1994; Menger and Keiper, 1998). These studies reveal the physical properties of the membranes through the calculation of the elementary deformation parameters. It is interesting to remark that all of these studies are mainly done in the liquid crystalline phase of pure phospholipid GUVs or in the presence of cholesterol because the fluid phase is the natural state of biological membranes. Since the early work of Harbich et al., which studied lecithin membrane melting with an optical microscope, a number of investigations have been done to visualize directly the effect

Received for publication 18 March 1999 and in final form 14 July 1999.

Address reprint requests to Dr. Luis A. Bagatolli, Laboratory for Fluorescence Dynamics, 184 Loomis Lab., 1110 West Green, Urbana, IL 61801. Tel.: 217-244-5620; Fax: 217-244-7187; E-mail: lab@alecto.physics.uiuc.edu.

© 1999 by the Biophysical Society

0006-3495/99/10/2090/12 \$2.00

of the phase transition in giant phospholipid structures (unilamellar and multilamellar) composed of pure phospholipids (Harbich et al., 1976; Yager et al., 1982; Evans and Kwok, 1982; Needham and Evans, 1988; Decher et al., 1990). To our knowledge, only a few systematic studies of the structure and mechanical properties of GUVs formed by synthetic phosphatidylcholine phospholipid below, at, and above the main phase transition temperature (T_m) in pure water were published (Evans and Kwok, 1982; Needham and Evans, 1988). These studies used a micromechanical test that involved micropipette aspiration to measure thermoelastic properties of the liquid crystalline and gel phases in DMPC GUVs (Evans and Kwok, 1982; Needham and Evans, 1988). An important result of the Needham and Evans work is the development of a mechanical model for the ripple phase (P_β) that correlates well with the observed experimental mechanical behavior (Needham and Evans, 1988). A similar study using the same temperature range and experimental approach was reported in GUVs composed of mixtures of phosphatidylcholine phospholipids and cholesterol (Needham et al., 1988).

Fluorescence spectroscopy is a frequently used tool for the study of lipid systems. Among several fluorescent probes, the particular spectroscopic characteristics of the amphiphilic fluorescent probe 6-dodecanoyl-2-dimethyl-amino-naphthalene (LAURDAN) offer several advantages in the study of phase transitions and phase coexistence in lipid systems. A number of studies were done to characterize LAURDAN behavior at different lipid interfaces (see review articles by Parasassi and Gratton (1995), Parasassi et al. (1998), Bagatolli et al. (1997), and Bagatolli et al. (1998)). For example, in phospholipid vesicles, the LAURDAN emission maximum exhibits a 50-nm red shift in going from the gel to the liquid crystalline phase (Parasassi and Gratton, 1995; Parasassi et al., 1998). This LAURDAN spectroscopic difference between the gel and the liquid crystalline phases allows phase discrimination simply by using fluorescence intensity measurements. To quantify the LAURDAN emission spectral changes, the excitation generalized polarization (GP_{ex}) was defined (Parasassi et al., 1990). This function is sensitive to the lipid packing reflecting the water content and dynamics at the lipid interface (Parasassi and Gratton, 1995; Parasassi et al., 1998). It has been shown that LAURDAN does not preferentially partition in either the gel or the liquid crystalline phase. Recently, the measurements of LAURDAN GP_{ex} using scanning two-photon excitation fluorescence microscopy opened a new approach to the interpretation of microscopic pictures of lipid phases in cells and multilamellar vesicles (Yu et al., 1996; Parasassi et al., 1997). In particular, exploiting the photoselection effect due to the linear polarization of the excitation light, it was possible to discriminate between homogeneous phase and domain coexistence (Parasassi et al., 1997). In the present work we study the temperature behavior of individual GUVs formed by pure phospholipids, using scanning two-photon excitation fluorescence microscopy. Our strategy is based on monitoring

single GUVs during the temperature scan, using the LAURDAN intensity images, and we visualize directly from these images the LAURDAN GP_{ex} function, which provides information about the lipid phase state.

MATERIALS AND METHODS

Materials

LAURDAN was from Molecular Probes (Eugene, OR). 1,2-Ditridecanoyl-*sn*-glycero-3-phosphocholine (DTPC), 1,2-dimiristoyl-*sn*-glycero-3-phosphocholine (DMPC), 1,2-dipalmitoyl-*sn*-glycero-3-phosphocholine (DPPC), and cholesterol were from Avanti Polar Lipids (Alabaster, AL).

Methods

Vesicle preparation

Stock solutions of phospholipids and cholesterol were made in chloroform. The concentration of the lipid stock solutions was 0.2 mg/ml. For GUV preparation we followed the electroformation method first described by Angelova and Dimitrov (Angelova and Dimitrov, 1986; Dimitrov and Angelova, 1987; Angelova et al., 1992). We constructed a special chamber connected to a water bath that allowed us to grow GUVs at different temperatures (see Fig. 1). We performed the microscopy experiments in the same chamber during and after the vesicle formation, using an inverted microscope (Axiovert 35; Zeiss, Thornwood, NY). The following steps were used to prepare the GUVs: 1) We spread $\sim 3 \mu\text{l}$ of the lipid stock solution on each Pt wire under a stream of N_2 . To remove the residues of organic solvent we put the chamber in a liophilizer for ~ 2 h. 2) We sealed the bottom part of the cell with a coverslip and then added Millipore water ($17.5 \text{ M}\Omega/\text{cm}$), covering the Pt wires. The Millipore water was previously heated at the desired temperature (50°C for DPPC and DPPC/cholesterol 30 mol%, 35°C for DMPC, DMPC/cholesterol 30 mol% and DTPC). We connected the Pt wires to a function generator (Hewlett-Packard, Santa Clara, CA) for ~ 90 min, applying a low-frequency AC field (sinusoidal wave function with a frequency of 10 Hz with an amplitude of 3 V). After the vesicle formed, we turned off the AC field and proceeded with the temperature scan. The GUV yield was $\sim 95\%$, and the mean diameter size was $\sim 25 \mu\text{m}$. We used a CCD color video camera (CCD-Iris; Sony) in the microscope to follow the vesicle growth and to select one vesicle for further observations. The temperature was measured using a digital thermocouple (model 400B; Omega, Stamford, CT) with a precision of 0.1°C . The LAURDAN labeling procedure was done in two ways. Either we premixed the fluorescent probe with the lipids in chloroform or we added a small amount (less than $1 \mu\text{l}$) of LAURDAN in dimethyl sulfoxide after vesicle formation (final LAURDAN/lipid ratio 1:500 mol/mol in both cases). The sample behavior during the temperature scan was the same, independently of the labeling procedure. To check if the presence of LAURDAN affects the GUV behavior, we followed the GUVs with and without the presence of LAURDAN, using the CCD camera during the temperature scan. We observed the same GUV behavior with temperature independently of the presence or absence of LAURDAN. To check the lamellarity of the giant vesicles we image several vesicles (up to 20 vesicles in different regions of the Pt wires) labeled with LAURDAN, using the two-photon excitation microscope. We found that the intensities measured in the borders of different vesicles were similar, with an average intensity ratio close to 1 for all vesicles of a given area. We concluded that the vesicles are unilamellar, in agreement with previous observations of GUVs by the electroformation method (Mathivet et al., 1996).

Two-photon fluorescence measurements

GP_{ex} function

The LAURDAN emission spectrum is blue in the lipid gel phase. In the liquid crystalline phase the LAURDAN emission spectrum moves during

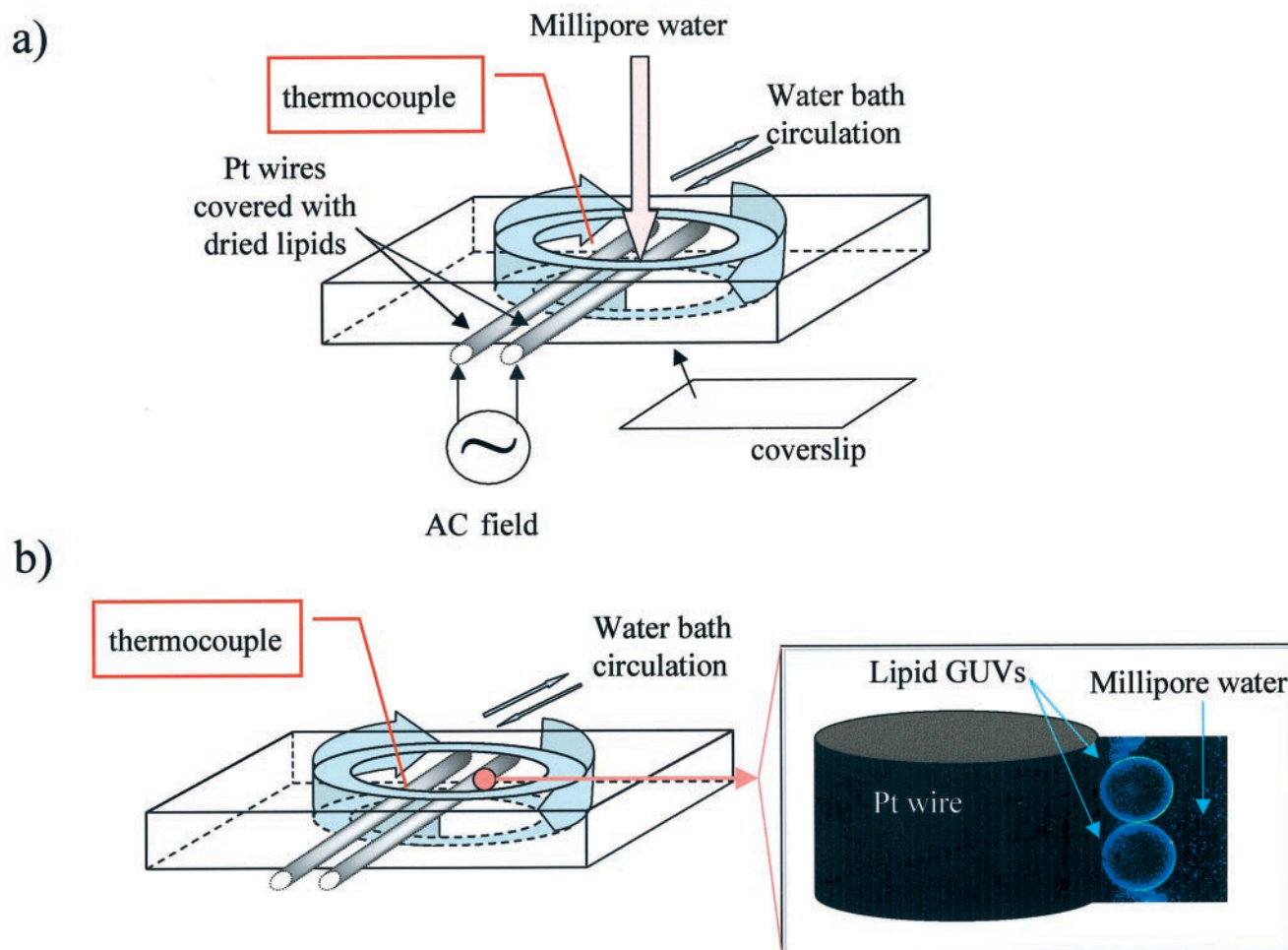


FIGURE 1 The sketch shows the chamber design for vesicle preparation before and after vesicle formation (*a* and *b*, respectively). The inset in *b* shows the vesicles in the chamber after the formation procedure. The water flux from the water bath is circulating in a plastic tube surrounding this module.

the excited-state lifetime from blue to green (Parasassi et al., 1990, 1991). To quantify the emission spectral changes, the excitation generalized polarization (GP_{ex}) function was defined analogously to the fluorescence polarization function as

$$GP_{ex} = \frac{I_B - I_R}{I_B + I_R}$$

In this function, the relative parallel and perpendicular orientations of the polarizer were replaced by the intensities at the blue and red edges of the emission spectrum (I_B and I_R , respectively), using a given excitation wavelength (Parasassi et al., 1990, 1991).

Experimental apparatus for two-photon excitation microscopy measurements

Two-photon excitation is a nonlinear process in which a fluorophore absorbs two photons simultaneously. Each photon provides half the energy required for excitation. The high photon densities required for two-photon absorption are achieved by focusing a high peak power laser light source on a diffraction-limited spot through a high numerical aperture objective. Therefore, in the areas above and below the focal plane, two-photon absorption does not occur, because of insufficient photon flux. This phe-

nomenon provides confocal capability without the use of emission pinholes. Another advantage of two-photon excitation is the low extent of photobleaching and photodamage above and below the focal plane. For our experiments we used a scanning two-photon fluorescence microscope developed in our laboratory (So et al., 1995, 1996). For the LAURDAN GP measurements we used a procedure similar to one previously described (Yu et al., 1996; Parasassi et al., 1997). We used an Axiovert 35 inverted microscope (Zeiss). The objective used in our experiments was a Zeiss 20× LD-Achroplan (0.4 N.A., air). A titanium-sapphire laser (Mira 900; Coherent, Palo Alto, CA) pumped by a frequency-doubled Nd:vanadate laser (Verdi; Coherent) was used as excitation light source with a 770-nm wavelength. The laser was guided by a galvanometer-driven *x-y* scanner (Cambridge Technology, Watertown, MA) to achieve beam scanning in both the *x* and *y* directions. A frequency synthesizer (Hewlett-Packard, Santa Clara, CA) controlled the scanning rate, and a frame rate of 9 s was used to acquire the three images (256 × 256 pixels) for the GP calculation. A polarizer attenuated the laser power to 50 mW before the light entered the microscope. The samples received about 1/10 of the incident power. Two optical band-pass filters (Ealing Electro-optics, Holliston, MA) with 46 nm bandwidth and centers at 446 and 499 nm were used to collect fluorescence in the blue and red regions of the LAURDAN emission spectrum. A miniature photomultiplier (R5600-P; Hamamatsu, Bridgewater, NJ) was used for light detection in the photon counting mode. A home-built card acquired the counts.

Vesicle image measurements

We obtained the images of the GUVs in the above-described chamber, using the Pt wires as a "holder." The vesicles were adsorbed to the Pt wires (that are covered by a lipid film) during the course of the experiment. The diameter of the vesicles was measured by using a calibration fluorescence standard. We determined that the pixel size in our experiments corresponds to $0.52\ \mu\text{m}$. We increased or decreased the temperature at a rate of $0.1^\circ\text{C}/\text{min}$. After the desired temperature was reached, we waited up to 10 minutes to allow the sample to equilibrate. Then we scanned the vesicles to obtain the two-photon images.

In a previous study Parasassi et al. showed that when polarized light is used to excite LAURDAN-labeled multilamellar vesicles, a photoselection effect operates in the fluorescence emission image (Parasassi et al., 1997). The transition dipole of LAURDAN in lipid vesicles is aligned parallel to the lipid chains (Parasassi and Gratton, 1995; Parasassi et al., 1998). Consider the linear polarization confined to the x - y plane. Exploring different sections of a spherical vesicle, we can observe that strong excitation occurs in the direction parallel to the excitation polarization, whereas poor excitation occurs in regions perpendicular to the excitation polarization (Fig. 2; Parasassi et al., 1997). In particular, this effect will be stronger in the x - y plane that passes through the center of the vesicle. If we observe the top or bottom regions of a spherical lipid vesicle we will find poor excitation. In addition, this effect depends on the phase state of the phospholipids. In the gel phase, the ordered packing of the lipid molecules increases the photoselection effect (Fig. 2 *a*). In the liquid crystalline phase, because of the low lipid order, we expect to have a component of the transition dipole of LAURDAN parallel to the excitation polarization. As a consequence, there is a difference in the emission intensity between the parallel and perpendicular orientations of the LAURDAN transition dipole (Fig. 2 *a*). In Fig. 2 *b* we show how the rotation of the polarized excitation light in the x - y plane affects the emission intensity pattern in the vesicle section image. This result strongly supports previous observations of the LAURDAN dipole orientation in the lipid membrane and shows the photoselection effect. A important point is that polarized light, which photoselects well-oriented LAURDAN molecules, also selects LAURDAN molecules associated with high GP_{ex} values (Parasassi et al., 1997). With the use of polarized excitation, when the image contains separate domains (pixels) of different GP_{ex} values, the higher GP_{ex} value domains appear parallel to the excitation polarization while the low GP_{ex} region is aligned perpendicular to the excitation polarization orientation (Fig. 2 *c*, *top*). 2) The lipid domains and the pixel have similar sizes. In this case the high GP_{ex} regions are again aligned parallel to the excitation polarization orientation. Instead the low GP_{ex} domains present a homogeneous distribution around the vesicle contour (Fig. 2 *c*, *center*). 3) The lipid domains are larger than the pixel size. Clearly separated GP_{ex} regions should be observed (Fig. 2 *c*, *bottom*).

RESULTS

We observed during the cooling cycle that the GUVs always remain spherical. At temperatures very close to the main phase transition ($\sim T_m - 1^\circ\text{C}$) during the cooling cycle, we observed a sudden movement like a shaking of the whole vesicle, in agreement with previous observations made in multilamellar vesicles (Yager et al., 1982). Immediately after this process we observed that a considerable percentage of vesicles detach from the platinum wires and migrate into the bulk solution. This behavior was independent of the

chain length of the synthetic phosphatidylcholine phospholipids used to form the GUVs (DTPC, DMPC, or DPPC). We measured the diameter of several single GUVs formed by pure DMPC and DPPC, during the cooling cycle. We observed that during the phase transition the vesicles showed a slight increase in the diameter ($\sim 1\%$), followed by a decrease in the diameter of $\sim 7\%$ after the vesicles reached the gel phase (Fig. 3, *a* and *b*, for DPPC and DMPC, respectively). All of the observed vesicles showed the increase in the diameter at the phase transition temperature. However, a small percentage of GUVs shows a slightly high decrease in diameter from the liquid crystalline to the gel phase (around 10%). The same observation was made in the case of DTPC (not shown). In the case of GUVs formed by DPPC we found a kink in the decrease in vesicle diameter at temperatures corresponding to the phospholipid pretransition (Fig. 3 *a*). In the case of DMPC we observed this kink, but it was located few degrees above the pretransition temperature (Fig. 3 *b*).

When we increased the temperature after cooling, a dramatic shape change was observed in the GUVs at the phase transition. We found this behavior not to be dependent on the phospholipid chain length, i.e., in GUVs formed by DTPC, DMPC, or DPPC. At the main phase transition temperature range the vesicles follow a sequence of different shapes as the temperature is increased, as follows: spherical-polygonal-ellipsoidal. After the phase transition temperature and during the heating cycle, we also observed shape changes in the GUVs from ellipsoidal to stomocyte (not shown). The first step in the sequence of vesicle shape transformations, the spherical to polygonal shape transition, occurs in a very narrow temperature range, i.e., during the gel-to-liquid crystalline phase transition (coexistence of lipid domains) (Fig. 4). At this temperature we observed fluctuations of the membrane borders. We found that this process is largely independent on the temperature scan rate. As shown in Fig. 4, the planar parts of the vesicles disappear as we raise the temperature to finally reach the ellipsoidal shape. The polygonal shape state is stable in time if we maintain the temperature at T_m . All of the processes observed during the cooling and heating cycles at the phase transition temperature were reversible.

We performed the same temperature cycle experiments with GUVs formed by DPPC or DMPC with $30\ \text{mol}\%$ of cholesterol. All of the above-described processes at the phase transition temperature range were absent in the samples containing cholesterol (see Fig. 5). We only observed shape changes in the cholesterol-containing GUVs during the heating cycle above and far from the pure phospholipid main phase transition, which were like spherical-to-ellipsoidal shape changes, but without the presence of the polygonal shape (Fig. 5).

We measured the phase state of single vesicles, using the LAURDAN GP_{ex} function. The LAURDAN GP_{ex} values obtained during the temperature scan in GUVs are consistent with those found in previous studies of multilamellar vesicles, using steady state fluorescence (see Fig. 3;

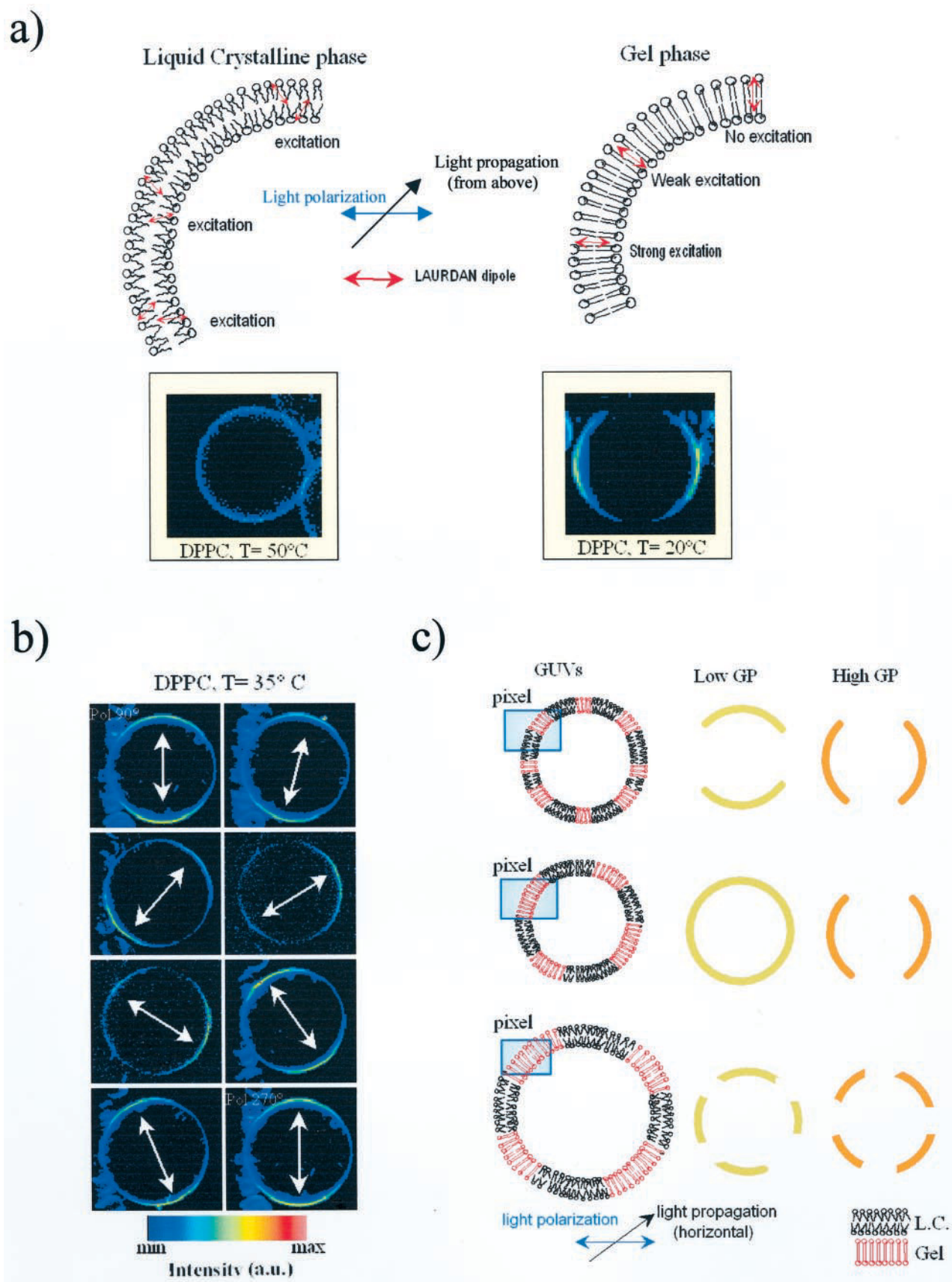


FIGURE 2 Schematic representation of the photoselection effect, using LAURDAN in GUVs. (a) LAURDAN transition dipole orientation in the bilayers and emission intensity pattern in a section of a single GUV in the gel and fluid phases. (b) The effect of rotating the polarization of the excitation light in the gel phase. (c) GP_{ex} pattern in vesicles assuming phase coexistence by the effect of the photoselection for different domain sizes.

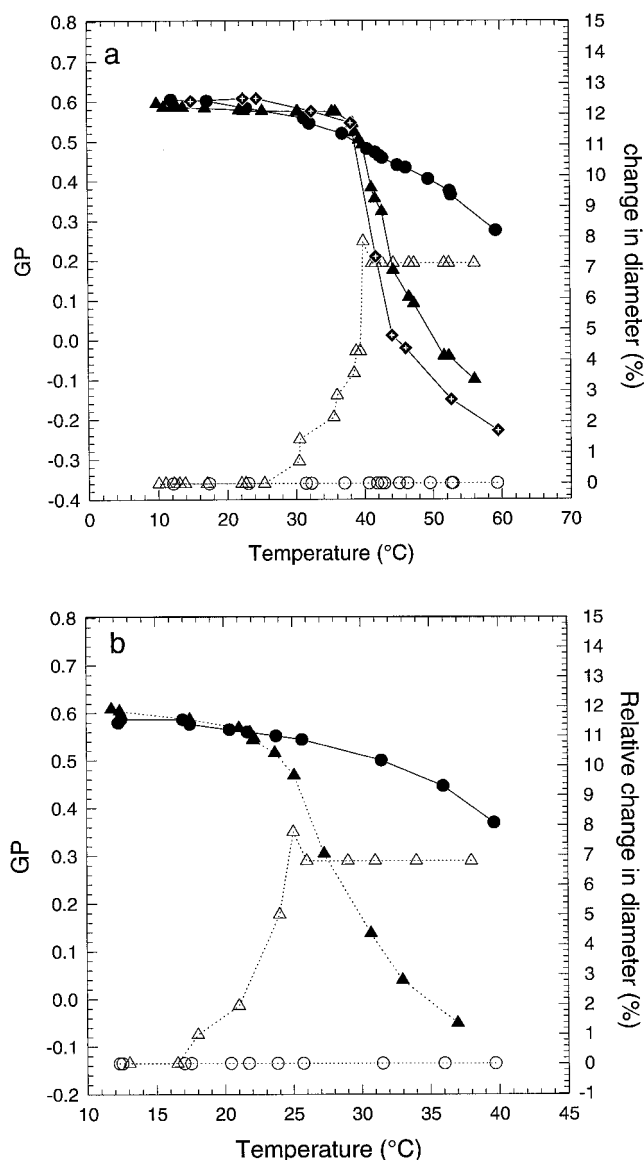


FIGURE 3 LAURDAN GP_{ex} and fractional change of diameter versus temperature of GUVs formed by DPPC and DPPC/cholesterol 30 mol% (a) and DMPC and DMPC/cholesterol 30 mol% (b) during the cooling cycle. Filled symbols correspond to GP_{ex} versus temperature, and empty symbols correspond to relative change in diameter versus temperature. (a) \blacktriangle , \triangle , DPPC; \bullet , \circ , DPPC/cholesterol 30 mol%; \blacklozenge , DPPC multilamellar vesicles. (b) \blacktriangle , \triangle , DMPC; \bullet , \circ , DMPC/cholesterol 30 mol%.

Parasassi et al., 1991). However, the phase transition of a single GUV is broader and the phase transition temperature is shifted to higher temperatures compared to that observed in phospholipid multilamellar vesicles obtained by conventional cuvette steady-state fluorescent measurements. Fig. 3 a shows the comparison between the phase transition in multilamellar vesicles and a single GUV composed by DPPC. The same behavior was observed in DMPC and DTPC GUVs (not shown). To explore the lipid heterogeneity during the temperature scan we exploited the photo-selection effect due to the linear polarization of the excitation light previously reported for LAURDAN in multilamellar

vesicles (see Materials and Methods and Parasassi et al., 1997). Fig. 6 shows the LAURDAN GP_{ex} images and GP_{ex} histograms, respectively, in a single DPPC GUV above, at, and below the main phase transition temperature during the cooling cycle. In the liquid crystalline phase we observed a broad LAURDAN GP_{ex} histogram (Fig. 6 b) similar to that described previously for multilamellar vesicles (Parasassi et al., 1997). The microscopic image of the GUV shows disjoint regions, with the high GP_{ex} values regions located parallel to the direction of the polarization of the light and the low GP_{ex} values regions located perpendicular to the polarization of the light (see Fig. 6). This picture agrees with the observations made previously in multilamellar vesicles (Parasassi et al., 1997). At temperatures corresponding to the phase coexistence, the GP_{ex} images of pure phospholipid GUVs show disjoint regions of high and low GP_{ex} , similar to that found in the liquid crystalline phase (Fig. 6). Finally, in the case of the gel phase we observed a narrow LAURDAN GP_{ex} histogram with a marked photo-selection effect in the vesicle GP_{ex} image (see Fig. 6). Unfortunately, we were not able to calculate the GP_{ex} function during the polygonal shape for technical reasons due to the fluctuations in the borders of the membrane during the heating cycle. However, following the LAURDAN intensity with the blue band-pass filter (which selects preferentially the intensity coming from the phospholipid gel phase), we saw that the intensity coming from the flat parts was higher than that coming from the corners (see Fig. 4). Therefore, we concluded that the flat parts corresponded to gel regions, whereas the corners corresponded to fluid regions. As judged by the GP_{ex} profile measured during the cooling cycle and the temperature measured for the onset of the polygonal shape state, we did not observe temperature hysteresis at the main phase transition.

DISCUSSION

First we want to point out some differences between our observations and previously published ones about the shape behavior of the GUVs during the temperature scan. In experiments by Needham and Evans using the pipette aspiration method, they point out that, during the first cooling cycle, the GUVs suffer a rapid buildup of thermoelastic stress in the membrane, followed by vesicle rupture (Needham and Evans, 1988). Before the temperature cycle, the authors resealed the ruptured GUVs, raising the temperature to the main phase transition and obtaining vesicles with sufficient excess area (over that of a sphere of equivalent volume) to pass through the phase transition unstressed (Needham and Evans, 1988). In the work done by Meléard et al., using DMPC GUVs obtained by the electroformation technique, they observed two different behaviors of GUVs by passing through the main phase transition during the cooling cycle. In one case the GUVs showed an “explosion” process (the liposomes being destroyed) at the phase transition temperature. In the other case the GUVs passed

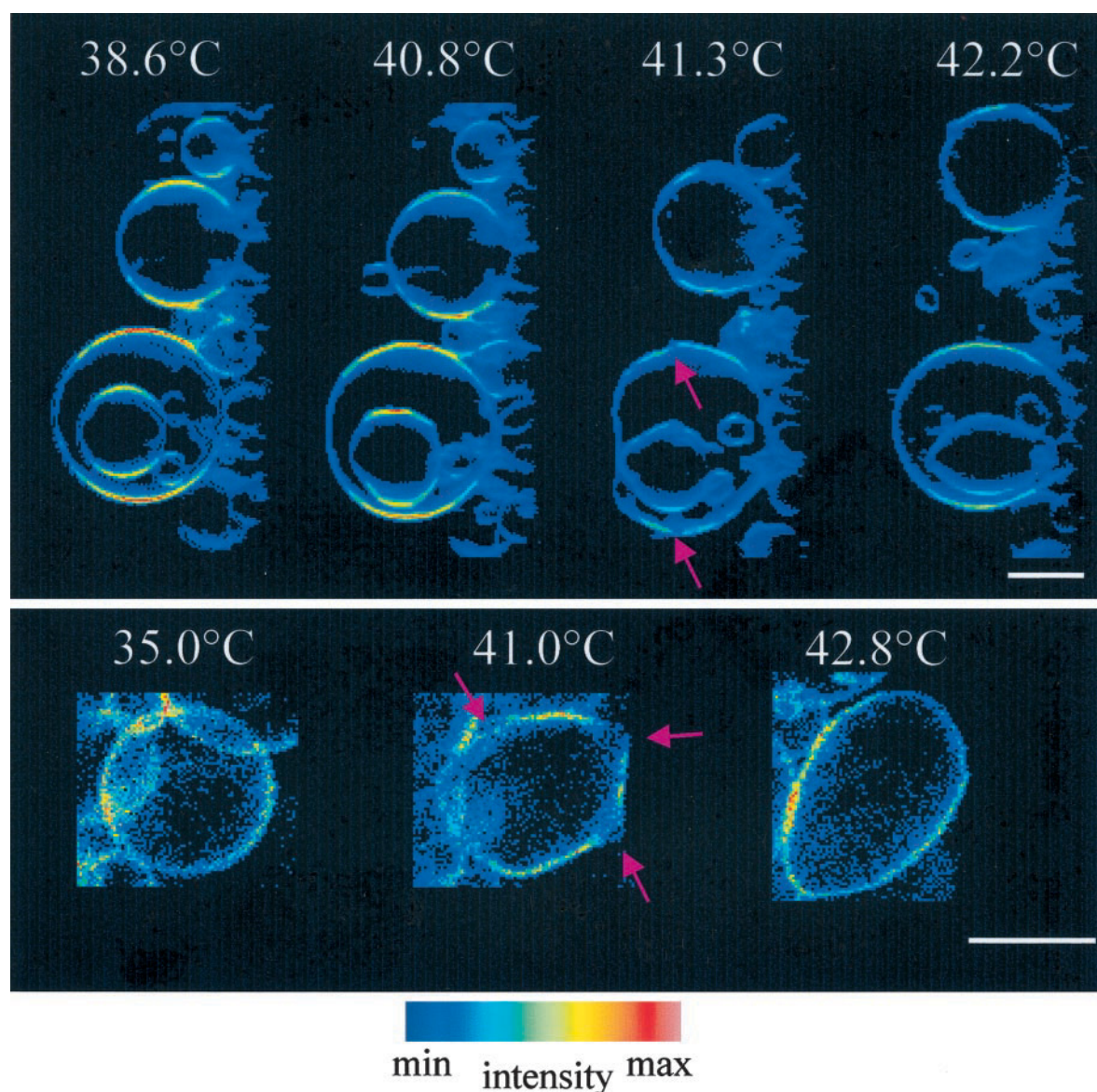


FIGURE 4 Shape changes in DPPC vesicles during passage through the main phase transition during the heating cycle. The images show LAURDAN intensity in a false color representation. The bars correspond to 20 μm . The same effect was found in DTPC and DMPC. The pink arrows show the low intensity (fluid) regions (see text).

through the main phase transition, assuming a nonfluctuating spherical shape stable at low temperatures (below the phase transition) (Meléard et al., 1997). In our experiments, using GUVs formed by pure DPPC, DMPC, or DTPC, we found that the vesicle shape always remained spherical at temperatures below the main phase transition, in agreement with one of the observations made by Meléard et al. (1997). However, we did not observe an explosion of the GUVs, and we did not find vesicle rupture at the main phase transition temperature during the cooling cycles. Furthermore, we followed the shape behavior of GUVs that detach the platinum wires, and again we did not find explosion of vesicles during the cooling cycle. In our system the vesicles are tightly adsorbed to the lipid films that cover the platinum wires, avoiding interaction with other materials (for

example, glass). This fact allows us to follow the temperature behavior of the vesicles in an easy and unperturbed way under the microscope.

GUVs shape hysteresis at the phase transition temperature: cooling and heating cycles

Our observation about the vesicle diameter overshoot at the phase transition during the cooling cycle allows us to propose a model to explain the effect of lipid domain coexistence on the average vesicle's "macroscopic" properties. We propose that at the main phase transition temperature between the fluid and gel domains there are defects that allow water to flow throughout the membrane, a process necessary

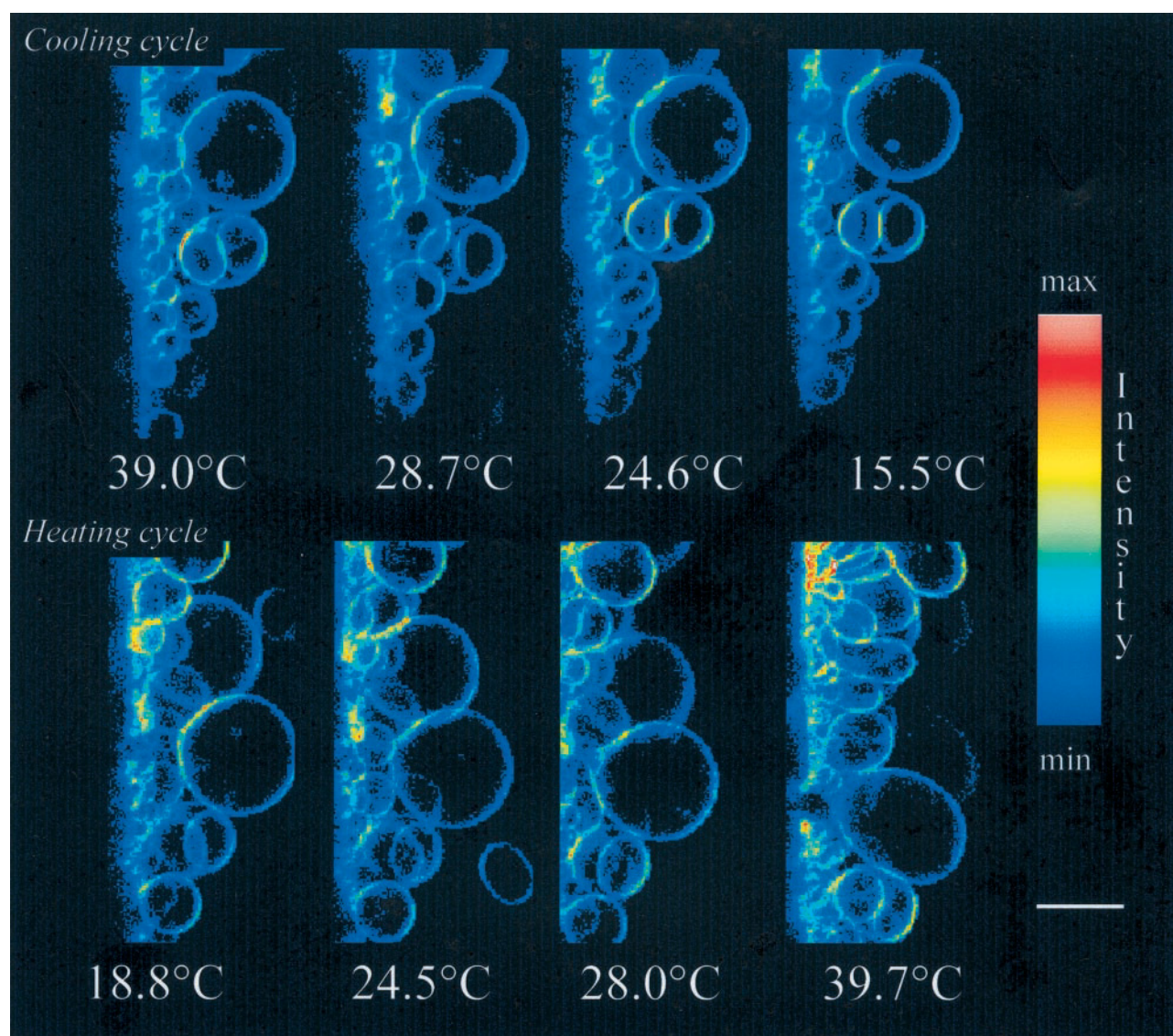
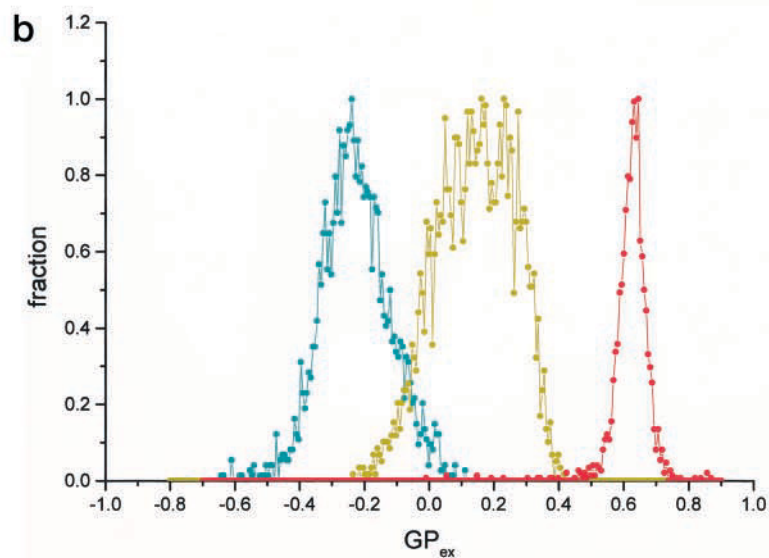
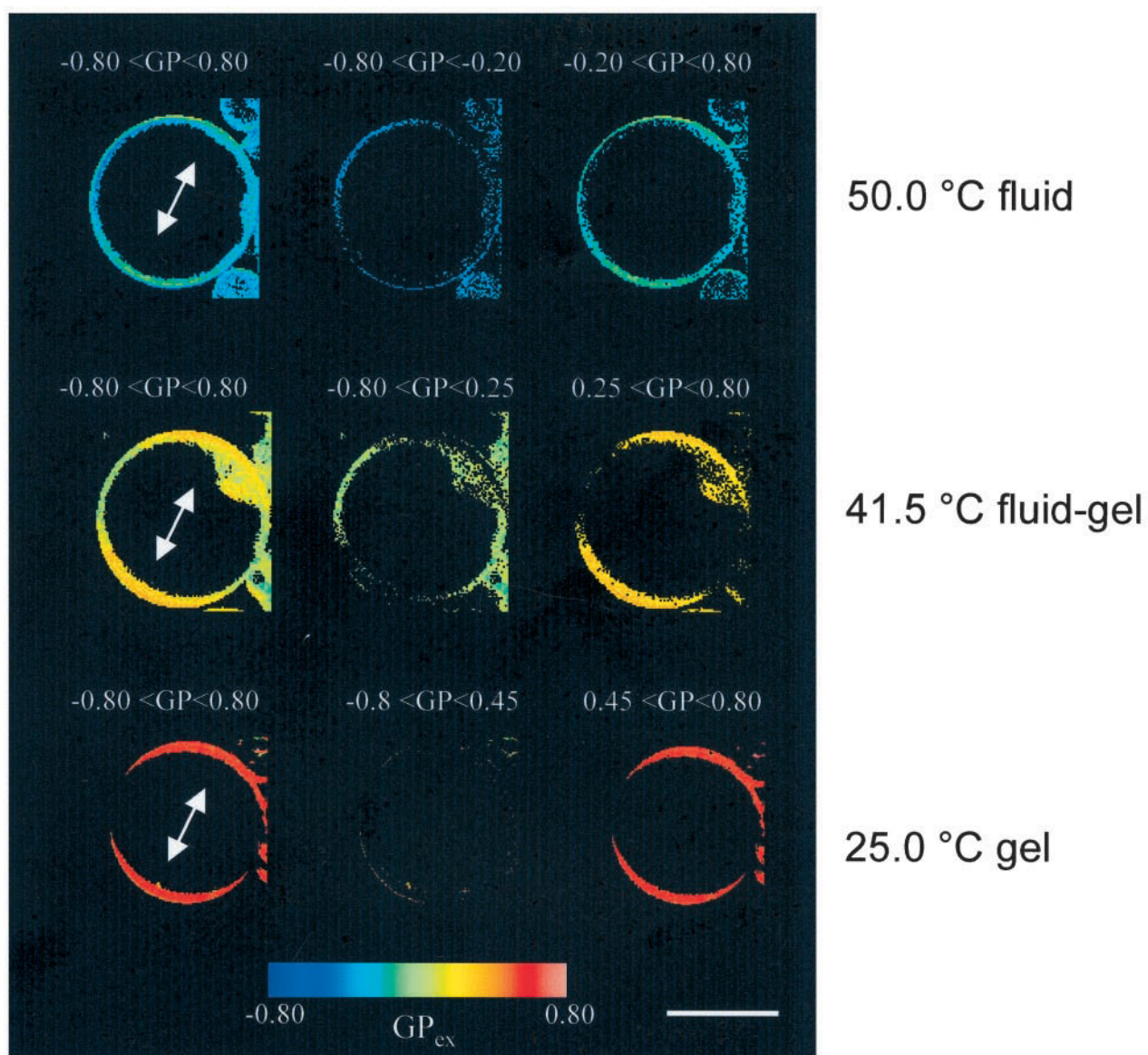


FIGURE 5 The effect of the heating and cooling cycles on the shape of GUVs formed by DMPC/cholesterol 30 mol%. The images show LAURDAN intensity in a false color representation. The bars correspond to 20 μm . The same effect was found in GUVs formed by DPPC/cholesterol 30 mol%.

for the change of the vesicle diameter. Our hypothesis is in keeping with some considerations by Mouritsen and Zuckermann about the softening of lipid bilayers at the phase transition temperature (Mouritsen and Zuckermann, 1985). They pointed out, using computer simulations, that at the phase transition there are strong density fluctuations that increase the possibility of pore formation in the membrane, accompanied by long-lived cluster distributions. The occurrence of clusters implies the presence of a substantial fraction of interfacial regions, which facilitate passive permeation of matter (Mouritsen and Zuckermann, 1985). The presence of long-lived domains with soft walls, characterized by less effective packing of the lipid acyl chains, might create a leakage of small molecules (Mouritsen and Zuckermann, 1985).

During the cooling cycle and after the phase transition the vesicle's diameter decreased by $\sim 7\text{--}8\%$. A small drop in the diameter at temperatures corresponding to the lipid

pretransition was observed in DMPC and DPPC GUVs. The change in diameter corresponds to a decrease in the area of $\sim 13\text{--}15\%$. These results are similar to those obtained by Needham and Evans in DMPC GUVs, who used the microaspiration test, applying moderate stress level on the lipid membrane (Needham and Evans, 1988). In this case the authors concluded that the rippled phase ($P_{\beta'}$) is prevented and the vesicles pass from the L_{α} phase to a metastable phase that they termed L_{β}^* , to finally reach the $L_{\beta'}$ phase. They assume the L_{β}^* phase to be planar crystalline, with the lipid acyl chains tilted to the bilayer normal, as in the low-temperature $L_{\beta'}$ phase (Needham and Evans, 1988). In the case of vesicles under low stress, these authors observed that the vesicles pass to the rippled phase with a change in area of $\sim 20\%$ (Needham and Evans, 1988). We can observe this behavior in a small fraction of the GUV population in our measurements. Therefore, we conclude that in our samples the majority of the GUV population can

a

be stressed without rupture by the temperature changes. This observation is important for the “natural” evolution of the sample with temperature, considering that in our system we did not pretreat the GUVs like these authors did in their work (see above, Needham and Evans, 1988). On the other hand, these authors did not report the overshoot in the vesicle area at the main phase transition temperature during the cooling cycle, as we did in our experiments.

In our experiments, during the heating cycle, it was not possible to measure the changes in the vesicle diameter because of the changes in the shape of the GUVs and the appearance of the polygonal shape (see Fig. 4). With respect to this point Meléard et al. reported that immediately above the phase transition, during the heating cycles, the GUVs formed by DMPC resembled an ellipsoid, showing membrane fluctuations, in agreement with our observations (Meléard et al., 1997). However, they did not mention the presence of the polygonal shape, which precedes the GUV ellipsoidal shape, observed in our experiments during the heating cycle. With regard to the microscopic picture of the GUV polygonal shape, we concluded that gel-phase regions of the lipid bilayer become planar, and the vesicle bends along fluid line defects formed by liquid crystalline domains at the phase transition. In our two-photon excitation images the corners clearly correspond to the liquid domains, whereas the flat parts correspond to the gel domains, as judged by the different intensity of the LAURDAN emission when observed throughout the blue filter. With regard to this observation, Sackmann and Feder reported a picture with flat walls in small vesicles composed of mixtures of DMPC/DMPE in the region of domain coexistence (Sackmann and Feder, 1995).

A major question remains as to the physical mechanism responsible for the formation of the polygonal vesicle shape at the transition temperature. While a model of this shape transition is beyond the scope of this article, we point out some possible contributions to this process: 1) During the heating cycle, the gel-phase regions are stressed by the curvature imposed by the spherical shape of the vesicles. When there is enough fluid phase, some parts of the vesicle still in the gel phase can assume a planar geometry to release tension due to the curvature. Instead, the curvature is taken by the fraction of fluid regions, which are confined along the polygonal lines. 2) During the heating cycle, water must penetrate into the vesicle to accommodate the larger diameter corresponding to the fluid phase. However, unless a pore is formed, the vesicle cannot expand. To accommodate the larger surface area with the same volume the vesicle must change shape—for example, assume a polygonal shape. When a large enough pore is produced, the vesicle can relax to the spherical shape. 3) The process

described in 2) is different during the cooling cycle. Now water must leave the vesicle interior to accommodate the smaller vesicle diameter corresponding to the gel phase. This condition can only be achieved by a spherically shaped vesicle. When a pore is formed, the water can exit the vesicle. This sudden flow may account for the shaking of the vesicle, which occurs at this temperature. In summary, the vesicle will attain whatever geometric shape is consistent with two constraints: 1) a given bilayer area and 2) a given interior volume, which is determined by the trapped water and the leakage rate across the membrane.

Another observation that we made in our system is the shape changes of the pure phospholipid GUVs (DTPC, DMPC, and DPPC) in the liquid crystalline phase during the heating cycle. We observed that the GUV shape changes from ellipsoidal to a stomocyte shape, in line with the observations in DMPC GUVs of Käs and Sackmann (1991). Furthermore, this behavior was observed in GUVs formed by the phospholipid/cholesterol mixture at high temperatures in the heating cycle. Concerning this particular type of transition, Käs and Sackmann pointed out that it can be explained in terms of the bilayer coupling model, assuming small differences in the thermal expansivities of the two monolayers (Käs and Sackmann, 1991).

The GUV shape hysteresis is abolished by the presence of 30 mol% cholesterol

An important result that supports our hypothesis about the effects of domain coexistence in the GUV structure is the behavior, during the cooling and heating cycles, of GUVs formed by mixtures of phospholipids (DMPC or DPPC) and 30 mol% cholesterol. In GUVs formed by the phospholipid/cholesterol mixture, the shape changes observed for pure phospholipid GUVs at the main phase transition temperature were absent. The absence of gel and fluid domains due to the well-known homogenizing effect of cholesterol in phospholipids bilayers explains our observations. The cholesterol experiment strongly indicates that the characteristics of the gel and liquid crystalline phase coexistence in GUVs formed by pure phospholipids is responsible for the processes observed at the phase transition temperature during the cooling and heating cycles (polygonal shape and diameter change, respectively).

The LAURDAN GP_{ex} function provides information about the lipid phases in a single GUV

We followed the phase transition of single GUVs formed by DTPC, DMPC, or DPPC, using the LAURDAN GP_{ex} func-

FIGURE 6 (a) LAURDAN GP_{ex} images of a single GUV composed by DPPC at 50°C (top), at 41.5°C (center), and at 25°C (bottom) during the cooling cycle. The white arrows indicate the orientation of the light polarization. The bar at the bottom right corner is 20 μm . (b) GP_{ex} histograms corresponding to the images presented in a: blue, 50°C; green, 41.5°C; red, 25°C. A similar pattern was obtained in DMPC and DTPC GUVs at temperatures above, at, and below the lipid phase transition.

tion during the cooling cycle. In the liquid crystalline state, we found a high heterogeneity in the GP_{ex} histogram values, in line with previous observations made in multilamellar vesicles composed of 1,2-dioleoyl-*sn*-glycero-3-phosphocholine (DOPC) or 1,2-dilauroyl-*sn*-glycero-3-phosphocholine (DLPC) (Parasassi et al., 1997). We also observed this heterogeneity in the LAURDAN GP_{ex} histogram in DLPC or 1-palmitoyl,2-oleoyl-*sn*-glycero-3-phosphocholine (POPC) single GUVs (not shown). LAURDAN is sensitive to the water content in phospholipid interfaces (Parasassi and Gratton, 1995; Parasassi et al., 1998). To explain the heterogeneity of the LAURDAN GP_{ex} values in the liquid crystalline phase of DOPC and DLPC multilamellar vesicles at room temperature, Parasassi et al. proposed the following model. In the liquid crystalline phase there is a distribution of sites with different sizes in which the LAURDAN molecule can reside (Parasassi et al., 1997). The larger the number of water molecules in the site, the lower the GP_{ex} value and the larger the cavity around the LAURDAN molecule (Parasassi et al., 1997). This model explains very well our observations in GUVs above the main phase transition. Also in the work by Parasassi et al., the authors concluded that the domain size in the liquid crystalline phase was smaller than the microscope resolution (~ 200 nm), in agreement with our results. They proposed that the small size of the microdomains could arise either because along a single layer of the multilamellar vesicle the domains are small or because the layers are so close that the contribution from individual layers cannot be resolved. From our experiments in GUVs we can conclude that the domain size in the bilayer is smaller than the microscope resolution.

At the phase transition temperature of pure phospholipid GUVs and during the cooling cycle, disjoint regions in the GP_{ex} images clearly suggest the coexistence of gel and fluid domains of a size smaller than the microscope resolution. From the GP_{ex} histogram we conclude that the separation of the image in high and low GP_{ex} domains does not simply reflect large pure gel and liquid crystalline domains. Similar observations were previously reported by Parasassi et al. in multilamellar vesicles composed of DOPC/DPPC 1:1 mixtures at room temperature, where phase coexistence occurs (Parasassi et al., 1997). We want to remark that the nature of the GP_{ex} images found in pure phospholipid GUVs at the temperature of phase coexistence are independent of the chain length of the phosphatidylcholine phospholipid that forms the GUVs (DTPC, DMPC, and DPPC in our case). The observations made with the GP_{ex} during the cooling cycle about the domain size reflect only one aspect of the effect of the phase transition on the structure of the GUVs. The microscopic scenario changes during the heating cycle in pure phospholipid GUVs, as we show in Fig. 4. In this case, the size of the domains is visible as brighter and dimmer regions in the microscope pictures at the beginning of the phase transition. With an increase in temperature, a decrease in the size of the flat parts in the vesicle borders is observed. We predict that in multilamellar vesicles (MLVs) this effect will be more difficult to observe because of the

presence of multilayer arrangement. The interaction between layers could affect the formation of the polygonal shape.

Finally, in the gel phase the narrow GP_{ex} histogram reflects a homogeneous environment in line with the ordered lipid packing of the membranes. The last result is also in agreement with the observation made by Parasassi et al. in multilamellar vesicles in the gel phase (Parasassi et al., 1997).

The temperature transition region in GUVs is broader than MLVs

We found a broader phase transition temperature region in a single GUV with a slight increase in the T_m independent of the pure phospholipid composition (DTPC, DMPC, or DPPC), with respect to that found in MLVs (see Fig. 3 *a*). The increase in the T_m connected with a decrease in the curvature of the lipid bilayer was reported by Brumm et al. for mixtures of DMPC/DSPC and the pure components (Brumm et al., 1996). These authors show that the T_m presents the highest value in planar membranes (infinite curvature), while the lowest value is found in small unilamellar vesicles (SUVs). They point out that the increase in the membrane curvature lowered the lateral pressure of the lipid membrane, which accounts for the temperature shift (Brumm et al., 1996). The broadening of the phase transition observed in GUVs with respect to that found in MLVs is explained by the intrinsic differences between the structures of the GUVs and MLVs, i.e., the presence of multilayers in MLVs and their absence in GUVs. We believe that the high cooperative unit size is mainly responsible for the narrower phase transition in MLVs compared with that found in GUVs. As shown by Brumm et al., the transition of the MLVs is narrower than those found in SUVs and large unilamellar vesicles (LUVs) (Brumm et al. 1996).

Finally, we want to point out that we do not observe temperature hysteresis at the main phase transition. The transition temperature remains the same independently of the direction of the cycles, i.e., cooling or heating. Instead, we observed a "shape hysteresis" in GUVs. This GUV behavior reflects the average microscopic physical picture during the main phase transition of our pure phosphatidylcholine phospholipid samples. With our approach, we have the advantage of correlating the lipid phase with the shape behavior of the GUVs. Our results present a novel microscopic picture of the "natural" temperature evolution of lipid vesicles.

We thank Dr. J. D. Müller for help with the chamber design and for the chamber construction.

This work was supported by National Institutes of Health grant RR03155. LAB is a CONICET (Argentina) fellow.

REFERENCES

- Angelova, M. I., and D. S. Dimitrov. 1986. Liposome electroformation. *Faraday Discuss. Chem. Soc.* 81:303–311.

- Angelova, M. I., S. Soléau, Ph. Meléard, J. F. Faucon, and P. Bothorel. 1992. Preparation of giant vesicles by external AC fields. Kinetics and application. *Prog. Colloid Polym. Sci.* 89:127–131.
- Bagatolli, L. A., E. Gratton, and G. D. Fidelio. 1998. Water dynamics in glycosphingolipids studied by LAURDAN fluorescence. *Biophys. J.* 75:331–341.
- Bagatolli, L. A., B. Maggio, F. Aguilar, C. P. Sotomayor, and G. D. Fidelio. 1997. LAURDAN properties in glycosphingolipid-phospholipid mixtures: a comparative fluorescence and calorimetric study. *Biochim. Biophys. Acta.* 1325:80–90.
- Brumm, T., K. Jørgensen, O. G. Mouritsen, and T. M. Bayerl. 1996. The effect of increasing membrane curvature on the phase transition and mixing behavior of a dimiristoyl-*sn*-glycero-3-phosphocholine/distearoyl-*sn*-glycero-3-phosphocholine lipid mixture as studied by Fourier transform infrared spectroscopy and differential scanning calorimetry. *Biophys. J.* 70:1373–1379.
- Davenport, L., and P. Targowski. 1995. Long lived fluorescent probes for studying lipid dynamics: a review. *J. Fluorescence.* 5:9–18.
- Decher, G., H. Ringsdorf, J. Venzmer, D. Bitter-Suermann, and C. Weisgerber. 1990. Giant liposomes as model membranes for immunological studies: spontaneous insertion of purified K1-antigen (poly- α -2,8-NeuAc) of *Escherichia coli*. *Biochim. Biophys. Acta.* 1023:357–364.
- Dimitrov, D. S., and M. J. Angelova. 1987. Lipid swelling and liposome formation on solid surfaces in external electric fields. *Prog. Colloid Polym. Sci.* 73:48–56.
- Döbereiner, H. G., J. Käs, D. Noppl, I. Sprenger, and E. Sackmann. 1993. Budding and fission of vesicles. *Biophys. J.* 65:1396–1403.
- Epand, R. M. 1995. Comments on fluorescence methods for probing local deviations from lamellar packing. *J. Fluorescence.* 5:3–8.
- Evans, E., and R. Kwok. 1982. Mechanical calorimetry of large dimiristoylphosphatidylcholine vesicles in the phase transition region. *Biochemistry.* 21:4874–4879.
- Gratton, E., and T. Parasassi. 1995. Fluorescence lifetime distributions in lipid membrane systems. *J. Fluorescence.* 5:51–58.
- Harbich, W., R. M. Servuss, and W. Helfrich. 1976. Optical studies of lecithin-membrane melting. *Phys. Lett.* 57A:294–296.
- Käs, J., and E. Sackmann. 1991. Shape transitions and shape stability of giant phospholipid vesicles in pure water induced by area-to-volume changes. *Biophys. J.* 60:825–844.
- Koynova, R., and M. Caffrey. 1998. Phases and phase transitions of the phosphatidylcholines. *Biochim. Biophys. Acta.* 1376:91–145.
- Lasic, D. D. 1988. The mechanism of vesicle formation. *Biochem. J.* 256:1–11.
- Mabrey, S., and J. M. Sturtevant. 1976. Investigation of phase transition of lipids and lipid mixtures by high sensitivity differential scanning calorimetry. *Proc. Natl. Acad. Sci. USA.* 73:3862–3866.
- Mantsch, H. H., and R. N. McElhaney. 1991. Phospholipid phase transitions in model and biological membranes as studied by infrared spectroscopy. *Chem. Phys. Lipids.* 57:213–226.
- Mason, J. T. 1998. Investigation of phase transitions in bilayers membranes. *Methods Enzymol.* 295:468–494.
- Mathivet, L., S. Cribier, and P. F. Devaux. 1996. Shape change and physical properties of giant phospholipid vesicles prepared in the presence of an AC electric field. *Biophys. J.* 70:1112–1121.
- McElhaney, R. N. 1982. The use of differential scanning calorimetry and differential thermal analysis in studies of model and biological membranes. *Chem. Phys. Lipids.* 30:229–259.
- Meléard, P., C. Gerbeaud, P. Bardusco, N. Jeandine, M. D. Mitov, and L. Fernandez-Puente. 1998. Mechanical properties of model membranes studied from shape transformations of giant vesicles. *Biochimie.* 80: 401–413.
- Meléard, P., C. Gerbeaud, T. Pott, L. Fernandez-Puente, I. Bivas, M. D. Mitov, J. Dufourcq, and P. Bothorel. 1997. Bending elasticities of model membranes: influences of temperature and sterol content. *Biophys. J.* 72:2616–2629.
- Menger, F. M., and J. S. Keiper. 1998. Chemistry and physics of giant vesicles as biomembrane models. *Curr. Opin. Chem. Biol.* 2:726–732.
- Mouritsen, O. G. 1991. Theoretical models of phospholipid phase transitions. *Chem. Phys. Lipids.* 57:179–194.
- Mouritsen, O. G., and M. J. Zuckermann. 1985. Softening of lipid bilayers. *Eur. Biophys. J.* 12:75–86.
- Needham, D., and E. Evans. 1988. Structure and mechanical properties of giant lipid (DMPC) vesicles bilayers from 20°C below to 10°C above the liquid crystal-crystalline phase transition at 24°C. *Biochemistry.* 27: 8261–8269.
- Needham, D., T. M. McIntosh, and E. Evans. 1988. Thermomechanical and transition properties of dimiristoylphosphatidylcholine/cholesterol bilayers. *Biochemistry.* 27:4668–4673.
- Parasassi, T., G. De Stasio, A. d'Ubaldo, and E. Gratton. 1990. Phase fluctuation in phospholipid membranes revealed by LAURDAN fluorescence. *Biophys. J.* 57:1179–1186.
- Parasassi, T., G. De Stasio, G. Ravagnan, R. M. Rusch, and E. Gratton. 1991. Quantitation of lipid phases in phospholipid vesicles by the generalized polarization of LAURDAN fluorescence. *Biophys. J.* 60: 179–189.
- Parasassi, T., and E. Gratton. 1995. Membrane lipid domains and dynamics detected by LAURDAN. *J. Fluorescence.* 5:59–70.
- Parasassi, T., E. Gratton, W. Yu, P. Wilson, and M. Levi. 1997. Two photon fluorescence microscopy of LAURDAN generalized polarization domains in model and natural membranes. *Biophys. J.* 72:2413–2429.
- Parasassi, T., E. Krasnowska, L. A. Bagatolli, and E. Gratton. 1998. LAURDAN and prodan as polarity-sensitive fluorescent membrane probes. *J. Fluorescence.* 8:365–373.
- Sackmann, E. 1994. Membrane bending energy concept of vesicle and cell shapes and shape transitions. *FEBS Lett.* 346:3–16.
- Sackmann, E., and T. Feder. 1995. Budding, fission and domain formation in mixed lipid vesicles induced by lateral phase separation and macromolecular condensation. *Mol. Membr. Biol.* 12:21–28.
- So, P. T. C., T. French, W. M. Yu, K. M. Berland, C. Y. Dong, and E. Gratton. 1995. Time resolved fluorescence microscopy using two-photon excitation. *Bioimaging.* 3:49–63.
- So, P. T. C., T. French, W. M. Yu, K. M. Berland, C. Y. Dong, and E. Gratton. 1996. Two-photon fluorescence microscopy: time-resolved and intensity imaging in fluorescence imaging spectroscopy and microscopy. X. F. Wang and B. Herman, editors. Chemical Analysis Series, Vol. 137. John Wiley and Sons, New York. 351–374.
- Watts, A., and P. J. Spooner. 1991. Phospholipid phase transitions as revealed by NMR. *Chem. Phys. Lipids.* 57:195–211.
- Yager, P., J. P. Sheridan, and W. L. Peticolas. 1982. Changes in size and shape of liposomes undergoing chain melting transitions as studied by optical microscopy. *Biochim. Biophys. Acta.* 693:485–491.
- Yu, W., P. T. So, T. French, and E. Gratton. 1996. Fluorescence generalized polarization of cell membranes: a two-photon scanning microscopy approach. *Biophys. J.* 70:626–636.